FINAL REPORT

Exploiting EMI Signals During Active Transmission

SERDP Project MR-1659

AUGUST 2010

Gregory Schultz
Sky Research Inc.

REPORT DOCUMENTATION PAGE

Form Approved OMB No. 0704-0188

1. REPORT DATE (DD-MM-YYYY)	2. REPORT TYPE	3. DATES COVERED (From - To)
12-08-2010	Final Technical Report, V 2.0	02/12/2008-30/06/2010

4. TITLE AND SUBTITLE
Exploiting EMI Signals During Active Transmission
Final Technical Report

5a. CONTRACT NUMBER W912HQ-09-C-0003

5b. GRANT NUMBER

5c. PROGRAM ELEMENT NUMBER

6. AUTHOR(S)
Dr. Gregory Schultz, Sky Research, Inc.
Jonathan Miller, Sky Research, Inc.
Dr. Leonard Pasion, Sky Research, Inc.

5d. PROJECT NUMBER SERDP 1659

5e. TASK NUMBER

5f. WORK UNIT NUMBER

7. PERFORMING ORGANIZATION NAME(S) AND ADDRESS(ES)
Sky Research, Inc.
445 Dead Indian Memorial Road
Ashland, OR 9520

8. PERFORMING ORGANIZATION REPORT NUMBER

9. SPONSORING/MONITORING AGENCY NAME(S) AND ADDRESS(ES)
SERDP Program Office
Attn: Dr. Herb Nelson
901 North Stuart St.
Suite 303
Arlington, VA 22203

10. SPONSOR/MONITOR'S ACRONYM(S)

11. SPONSOR/MONITOR'S REPORT NUMBER(S)

12. DISTRIBUTION/AVAILABILITY STATEMENT
unlimited

13. SUPPLEMENTARY NOTES

14. ABSTRACT

Theoretically, signals measured during the transmit period (the "on-time") provide information about the instantaneous magnetization and current gathering in objects illuminated by a transmitter. In this SEED project, we examined the potential of on-time EMI data for improving the detection and discrimination of UXO and in rejecting clutter and noise. Through a combination of modeling and analysis of experimental data, we found that on-time data provide a number of theoretical and practical enhancements to aid in UXO characterization. This work also supported a more thorough understanding of the physical mechanisms being exploited by existing on-time instruments and their capabilities and limitations. We provide a theoretical basis that links our understanding of existing off-time pulsed induction and always-on frequency domain responses to the full waveform response. This approach provides for estimation of the magnetic properties of targets (e.g., demagnetization factors and bulk magnetic susceptibility) that are not obtainable with conventional off-time pulsed induction methods.

15. SUBJECT TERMS
electromagnetic induction sensors, on-time EMI transmitter signals, UXO

16. SECURITY CLASSIFICATION OF: a. REPORT	b. ABSTRACT	c. THIS PAGE	17. LIMITATION OF ABSTRACT	18. NUMBER OF PAGES	19a. NAME OF RESPONSIBLE PERSON
unclassified	unclassified	unclassified	unclassified	144	Dr. Herb Nelson

19b. TELEPHONE NUMBER (Include area code) 703-696-8726

Reset

Standard Form 298 (Rev. 8/98)
Prescribed by ANSI Std. Z39.18

EXECUTIVE SUMMARY

This project was undertaken by Sky Research Inc. and the University of British Columbia Geophysical Inversion Facility to examine the potential of exploiting electromagnetic induction (EMI) signals during active transmission - the so-called on-time.

Summary

Recent advances in EMI sensor capabilities have incorporated sensing mechanisms to more fully exploit the spatial response of UXO targets. These next generation systems utilize multi-axis and multi-static transmitter and receiver configurations to increase the spatial sampling of the scattered magnetic field response from targets for improved characterization. Previous research also has shown that enhanced capability may be gained from extending the temporal or spectral information. For example, characterization of a target's shape, size, and orientation can be improved by considering very early or late time decay information. Additionally, in-phase responses from frequency-domain metal detectors include magnetization effects that are not present in conventional time-domain systems. Similar information is also available in the time-domain by sampling the receiver waveform during the full period of both current "on" and "off" times. Since the introduction of high-rate digital sampling technology in EMI data acquisition, the whole waveform of measured EMI responses has been made available. The airborne electromagnetics community, in particular, has utilized full waveform EMI data to improve models of ground conductivity and magnetic susceptibility. Theoretically, received signals measured during the transmit period provide information about the instantaneous magnetization and current gathering in objects within the presence of the illuminating field. Although some work has been conducted to examine designs that provide for on-time signal reception, very few, if any, efforts have been concentrated on optimal methodologies for processing associated signals.

In this SEED project, we examined the potential of on-time EMI data for improving the detection and discrimination of UXO and to aid in rejecting anthropogenic and soil-related clutter and noise. Through modeling and simulation combined with experimental data collection and analyses, we found that on-time data provide a number of theoretical and practical enhancements to aid in UXO characterization. This work also supported a more thorough understanding of the physical mechanisms being exploited by existing on-time instruments and their capabilities and limitations.

Findings and Recommendations

In this project we have concentrated on providing a thorough and applied understanding of the utility of on-time responses. Our results suggest that processing of full waveform data (during both the transmitter "on" and "off" times) yield a number of benefits and should be pursued further. We provide a theoretical basis that links our understanding of existing off-time pulsed induction and always-on frequency domain responses to the full waveform response. This approach provides for estimation of the magnetic properties of targets (e.g., demagnetization factors and bulk magnetic susceptibility) that are not obtainable with conventional off-time pulsed induction methods. As has been shown previously, a comparison of on- and off-time signals lead to opposing polarity for purely ferrous and purely conductive objects - a simple, yet practical indicator of bulk material magnetization. In addition, we have shown that on-time signals may also yield important added information through their spatial response. For example, off-time responses over simulated spheres reveal an improved ability to resolve small, shallow targets relative to on-time. Conversely, on-time data are able to resolve deep, large targets, suggesting they are less influenced by surface ground clutter and provide added information for separating shallow and deep targets in a single region of interest.

Based on our preliminary findings, we recommend conducting a more thorough analysis of on-time signals and developing a test instrument to fully assess the utility of on-time data in target detection and discrimination. More work must be conducted on the analysis of both laboratory and field data to elucidate and validate the veracity and uniqueness of features extracted from on-time data. Physics-based features extracted from full waveform temporal signatures as well as their spatial evolution over targets will likely lead to better discrimination based on target size and aspect ratio as well as material composition and demagnetization effect.

Although a handful of on-time instruments exist, no current system fully leverages the potential advantages of full waveform EMI data. To do this, we suggest that advanced full waveform sensors be investigated, and, if warranted, developed into testable prototypes. In an idealized system, the current waveform would have the properties that maximize the magnetization effect on a target. Comparisons of basic waveforms lead to the suggestion of a linear ramp current excitation and rapid cessation as an ideal source for a full waveform system. This excitation characterizes the combined effect of a bipolar electromotive force (i.e., the electromotive force rapidly changes polarity as the ramp-on period transitions to the shut-off period) and a linear magnetic field applied to the target. The contrasting effects of the electromotive force and the magnetizing field produce a unique response that is a function of target features such as geometry, conductivity, and magnetic susceptibility.

The results of this project also suggest that an idealized system would likely utilize a current waveform with multiple ramp durations. The implementation of different ramp durations may allow for at least two different excitation periods. This approach provides certain advantages by: 1) enabling baseline excitation for comparing magnetization responses, 2) creating discrete energy states from which the secondary response decays, and 3) yielding needed information for cancelling the viscous magnetization effects of mineralized soils.

Perhaps the most critical design consideration for full waveform data acquisition is the ability to precisely null or cancel the primary magnetic field from the transmitter. Previous and on-going work on nulling designs for frequency-domain EM systems as well as digital cancellation methods applied to airborne EM survey data have strong leveraging potential. Geometric nulling using precise receiver positioning or gradient configurations have been used to cancel the primary field in frequency-domain EM instruments. Others have used digital cancellation methods by removing the component of the response that is aligned in phase with the transmitter. It is also common to use various modes of absolute field calibration for removing primary field effects. All of these methods have limitations, and we advocate an intelligent combination of methods that minimizes the impacts on sensitivity and dynamic range. Overlapping coil arrangements along with absolute calibration and balancing combined with digital cancellation and fine tuning with a Q-coil are likely the optimal choice for removing the primary field. We found that gradient configurations are less optimal due to their inherent fall-off in sensitivity with range.

6.1.1. B and dB/dt Measurement Methods

Our experimental setup included sensors that measure the B-field (wideband magnetic sensors) and those that sense the time rate of change of the magnetic field, or dB/dt, sensors (induction coils). For sensing dB/dt, coils of wire are used as the sensing elements to provide simple, low power, high-sensitivity at frequencies above a few hundred Hz. At lower frequencies, their sensitivity is reduced. Asten and Duncan (2007) list a number of potential benefits of B-field measurements including a higher sensitivity to large deep items compared to small shallow items. Our objective was not to rigorously determine the tradeoffs between B and dB/dt measurements during the on-time, but to provide example responses for both modalities.

B-field measurements were made with commercially-available giant magnetoresistive (GMR) magnetic field sensors. Magnetoresistive sensors use changes in resistance caused by an external magnetic field expressed as the percentage change in resistance per unit field or in voltage change out per volts in Oersteds. Magnetoresistance magnetometers are very attractive for low cost applications because they are simply energized by applying a constant current and the output voltage is a measure of the magnetic field. GMR sensors use layered metals consisting of thin ferromagnets that sandwich a thin conductor and an anti-ferromagnet to form a resistive bridge (specifically known as a spin valve). The technique relies on the ability of electrons to travel more easily either parallel to or perpendicular to the layers if the magnetizations of the two ferromagnets are parallel to each other. When the magnetizations are parallel, electrons undergo less scattering when going from an electronic band structure state in one of the ferromagnets into a similar state in the other ferromagnet.

We used the AA series analog GMR sensors from Non-volatile Electronics (NVE). The GMR sensor was combined with a small magnet to bias the measurement floor in order to overcome the Earth's field. Both the dB/dt coils and B-field GMR sensors were simultaneously logged with a National Instruments multi-channel data acquisition system with 16 bit resolution at sample rates up to 1.25 MHz. In general, raw data are displayed, although in some cases a simple low-pass filter has been applied to remove high frequency noise.

6.1.2. MPV Data

The Man-Portable Vector (MPV) instrument was used to collect data during both the transmitter on-time and after its rapid shut-off. This instrument was developed under SERDP MM-1443 project and is currently undergoing further enhancements. The MPV represents the next-generation of handheld UXO sensors and is unique in its ability to acquire multi-static and multi-component measurements over a programmable range of time channels. Details of the MPV instrument can be found in previous SERDP reports and literature (e.g., Barrowes et al, 2009).

During our experiments, MPV data was collected at Sky Research test facilities in Hanover, NH and in Vancouver, BC. The instrument was positioned off the ground on non-metallic stands in a benign area (minimum noise). A photograph of the basic test set-up is shown in Figure 38.

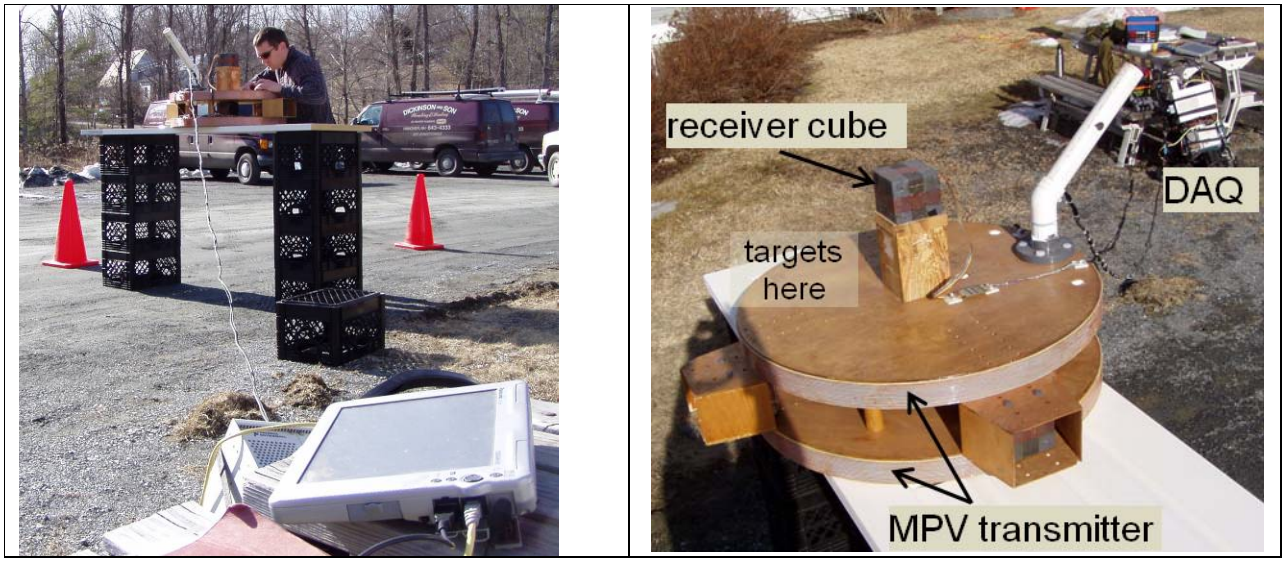

Figure 38. MPV data collection setup.

The primary field of the transmitter was reduced significantly (effectively nulled) by placing axi-symmetric targets in the approximate line of the maximum horizontal magnetic flux and acquiring measurements along the corresponding horizontal component receiver. A standard calibration procedure was also followed to correct for instrument drift and further cancellation of the primary field. The calibration background measurements were acquired often throughout our experiments. The transmitter generates an exponential on current with ramp on constant τ_a of ~5.5×10^{-4} s^{-1}. The ramp on time of the waveform reflects the charging circuit resistance and capacitance $\tau_a = RC$. For our data collection we utilized a 25 ms current on-time.

The first set of targets investigated consisted of coil loops of copper wire for which the L, R, and C parameters have been measured (Coils 1, 3, 8, and 9 - see Figure 29 above). The raw data as logged by the MPV are shown in Figure 39 (left side) over both the on- and off-time durations. The off-time behavior is as expected and reported elsewhere - the larger time constant loops exhibit longer decay, with generally predictable forms. The on-time signals yield the inductive response of the loops while the transmitter is ramping up current. Because the induced voltage in the receiver is proportional to emf in the coil, the on-time signals tend to reflect the time-derivative of the scattered field, which has a form that reflects the time-derivative of the current waveform.

Application of the analytical convolution model compares favorably with the measured MPV waveforms (Figure 39, right side). The current waveform was represented by an exponential ramp on with time constant of 5.5×10^{-4} s^{-1}. Both the on-time and off-time responses from the coil with the smallest time constant ($\tau = 7.8 \times 10^{-5}$ s^{-1}) were not predicted with same level of accuracy as the other coils.

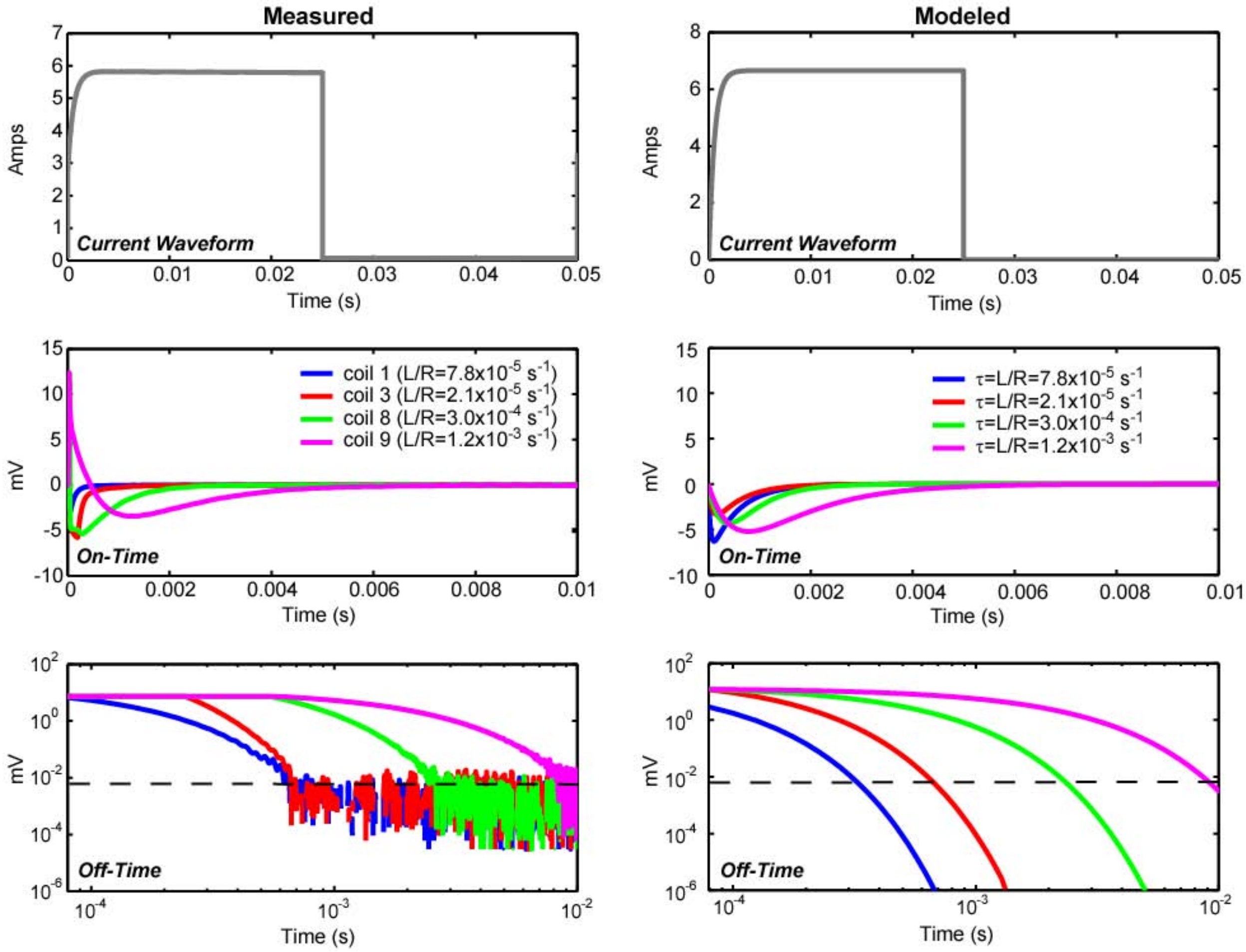

Figure 39. Measured (left) and modeled (right) on- and off-time responses from standard copper coil targets with varying time constants. The coil parameters are described in detail in Figure 30. In general, the convolution of a simulated exponential ramp on current waveform with a single time constant exponential decay impulse response predicts the on-time behavior.

Further MPV data were collected with solid aluminum and steel discs and cylinders. Targets were again placed where the z-component of the primary magnetic field was minimized. This provided an approximate primary field nulling in order to capture on-time responses. The corresponding on- and off-time responses are shown in Figure 40. The on-time responses for the solid cylinders (Figure 40-left-center) reveal opposing polarities as expected for targets dominated by inductive or magnetostatic effects. Similarly, but less obvious, the solid aluminum and steel discs (Figure 40-right-center) also exhibit opposing polarity during the on-time. This implies that the magnetic properties of the steel objects influence their on-time response. The disc-shaped objects have a decreased on-time response amplitude, further implying that volume magnetization is contributing significantly to the response.

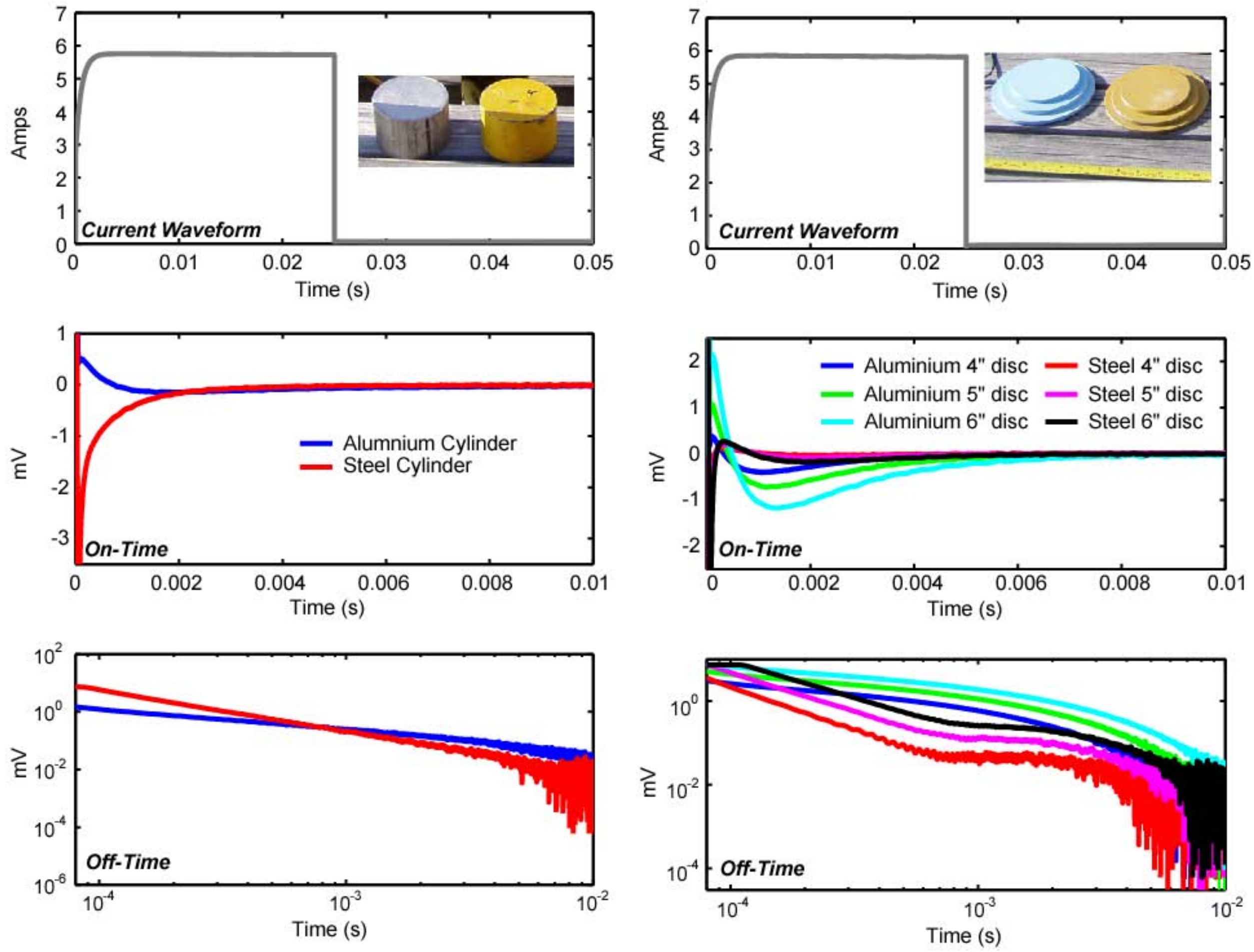

Figure 40. Measured current waveform (top panels), on-time responses (middle panels), and off-time responses (bottom panels) from solid axi-symmetric steel and aluminum objects. Comparisons between steel and aluminum cylinders (right) and thin discs (left) reveal the influence of volume magnetization on the on-time response.

In addition to the data acquired with cylindrical and disc-shaped objects, we also tested the MPV on-time response to varying orientation of a small steel rod (Figure 41- left). As expected, the steel rod generated the largest response along the axis of the strongest coupling with the primary field. Although, the object was positioned to remove the direct influence of the z-component (vertical) of the primary field, a z-oriented on-time response is still noticeable.

Experiments were also conducted with the MPV over the ground near the Sky Research test facilities in Hanover, New Hampshire. Although the soils are relatively benign with respect to mineralization or soil conductivity, a measureable response was observed by varying the height of the MPV over the ground. The on-time responses are shown in Figure 41 (right). The MPV was positioned on the ground and at increasing heights while recording its response during both on- and off-time durations. The strongest signal is observed when the sensor is located effectively on the ground and the signal decreases rapidly with standoff. We attempted to minimize the primary field by subtracting the response from the sensor elevated 1.10 meters (m) above the ground, forming an effective a simple, free-space calibration. Although the decay times are very short over the ground, the plot of the off-time response does not reveal a decay even at early times.

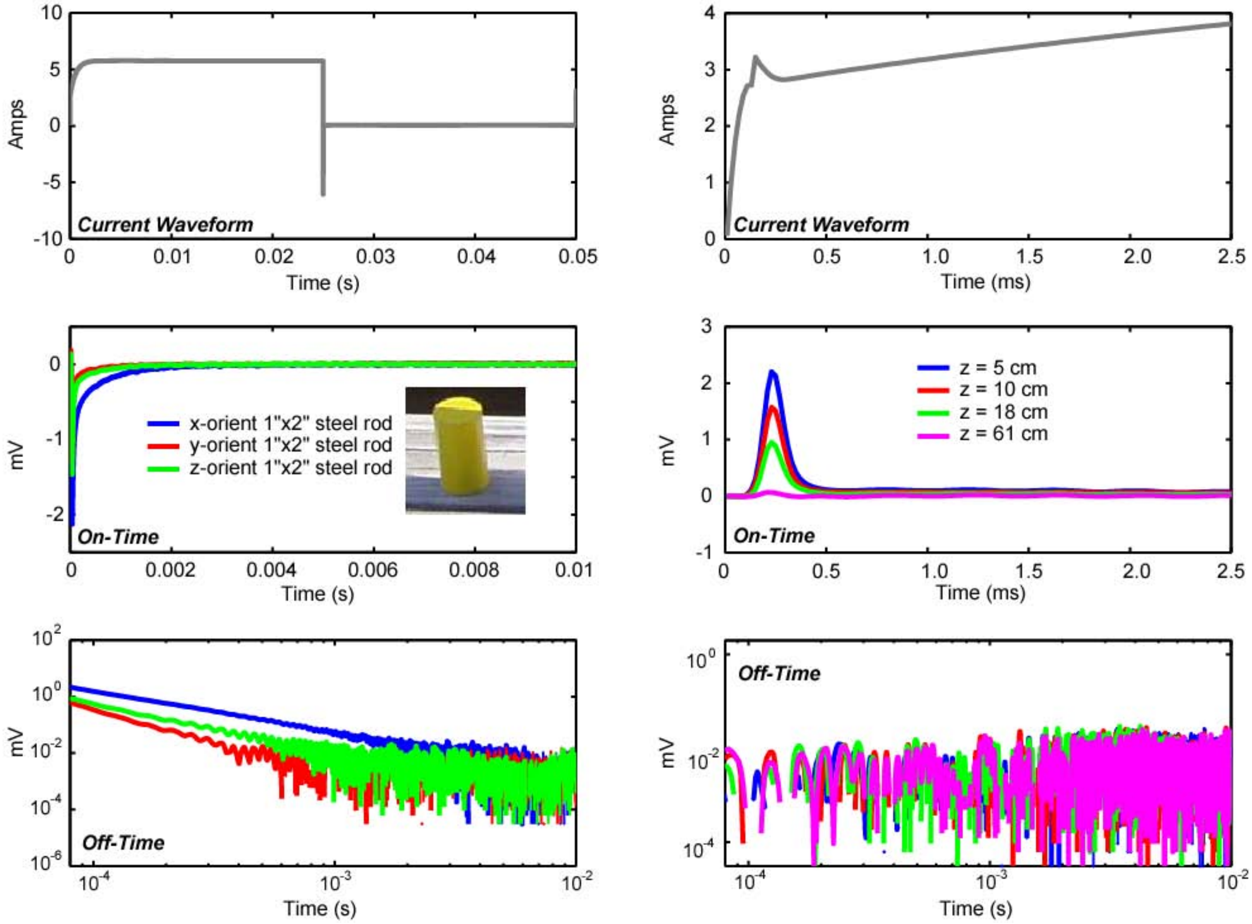

Figure 41. Measured current waveform (top panels), on-time responses (middle panels), and off-time responses (bottom panels) from a small solid steel rod (left) and over compacted soil (right). Slight differences between orientations of the steel rod are observable in both the on- and off-time responses. The maximum response is oriented along the primary coupling x-axis. Variable standoff from the soil generates a systematic on-time response, but is not noticeable in the off-time response. The time axis plotted for current waveform and on-time response correspond to the very short decay of the ground. Although, the current waveform has an anomalous current spike at ~200us, the soil response appears to react to only the driving emf and not the current spike.

A series of MPV on-time data were collected to assess the potential to discern solid metal cylinders from hollow ones. The experimental set-up is shown in Figure 42. The data are shown in Figure 43. Vertically oriented targets had a slightly stronger response. A small difference is observed between solid and hollow cylinders for both horizontally- and vertically-oriented targets.

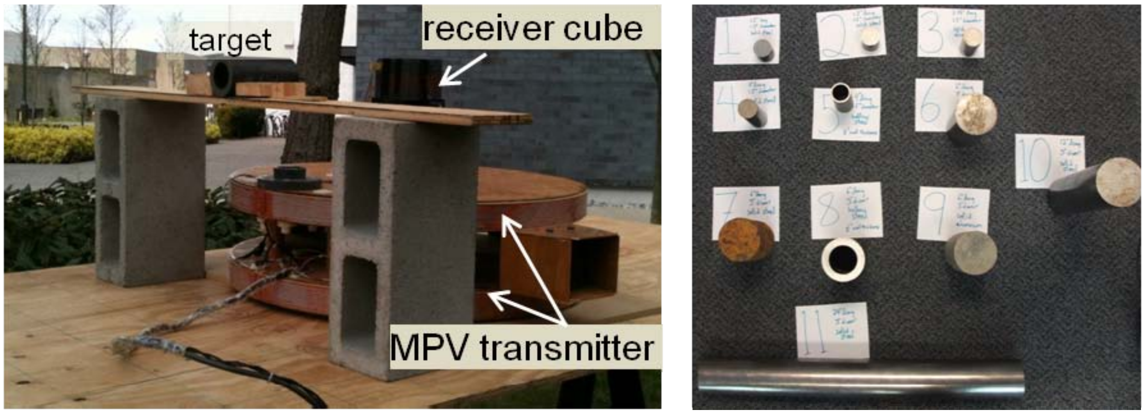

Figure 42. MPV data collection set-up for comparison of hollow and solid metal cylinders (left). Photograph of the targets used (right).

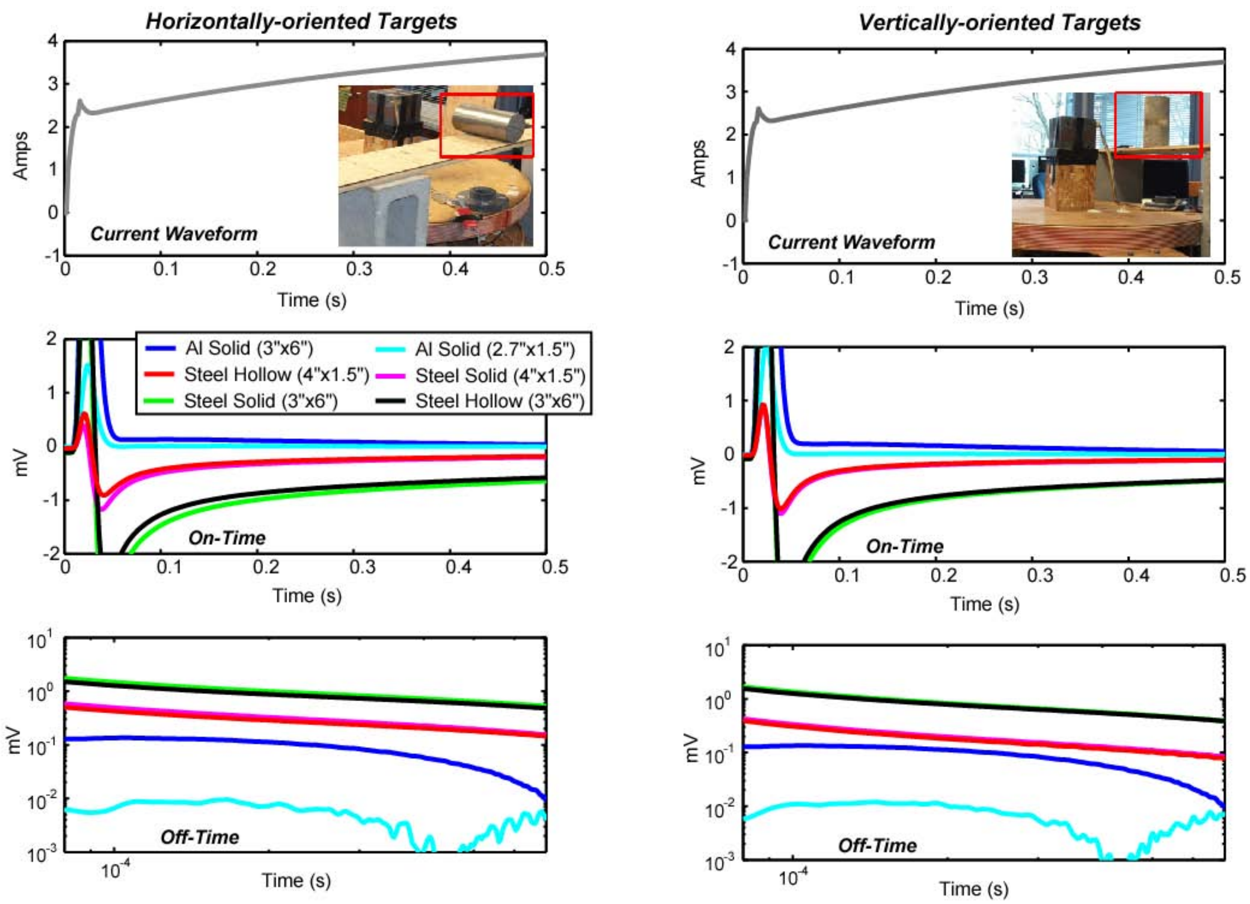

Figure 43 MPV data collection set-up for comparison of hollow and solid metal cylinders (left). Photograph of the targets used (right).

6.1.3. EM-61 Data

Controlled on-time data collection was also conducted using the Geonics EM-61 MkII transmitter. Like the MPV instrument, the EM-61 is a pulsed induction time-domain electromagnetic sensor utilizing and exponential current ramp-on waveform. The EM-61 MkII represents one of the most common commercial EM instruments used for UXO remediation. Therefore, it is of interest to assess how its current waveform and other features might be used to acquire on-time data.

The EM-61 current waveform has a duration of about 3.1 ms and a exponential ramp on constant τ_a of ~6.2×10^{-4} s^{-1}. The transmitter pulse repetition frequency is 75 Hz and peak power output is about 50 Watts with 25 Watts being the average power. Our initial set-up utilized a small 20 cm diameter winding of 200 turns of 22 gauge copper wire as a receiver. In addition, we also collected data with a GMR B-field sensor. No attempt was made to cancel the primary field. The basic experimental set-up is shown in Figure 44.

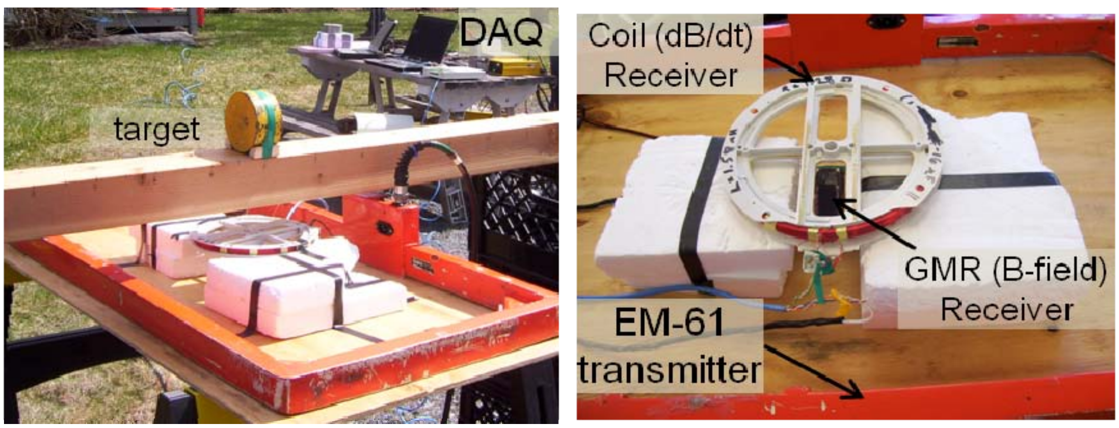

Figure 44. EM-61 data collection set-up with induction coil and GMR B-field sensor receivers.

Figure 45 and Figure 46 show the GMR (B-field) on-time response to the EM-61 transmitter excitation. Without any nulling of the primary field there is a distinguishable change in the signal when a metal cylinder is placed close to the receivers. The aluminum target appears to respond strongly to the transient emf during both the ramp-on and ramp-off periods relative to the background calibration data.

On-time data were also acquired with a differential receiver array allowing for cancelation of the primary field. A small frequency-domain array system containing 3 quadrapole receivers was used. The receiver pairs are wound in opposing directions and were centered inside the EM-61 transmitter. The experimental set up is shown in Figure 46 (right).

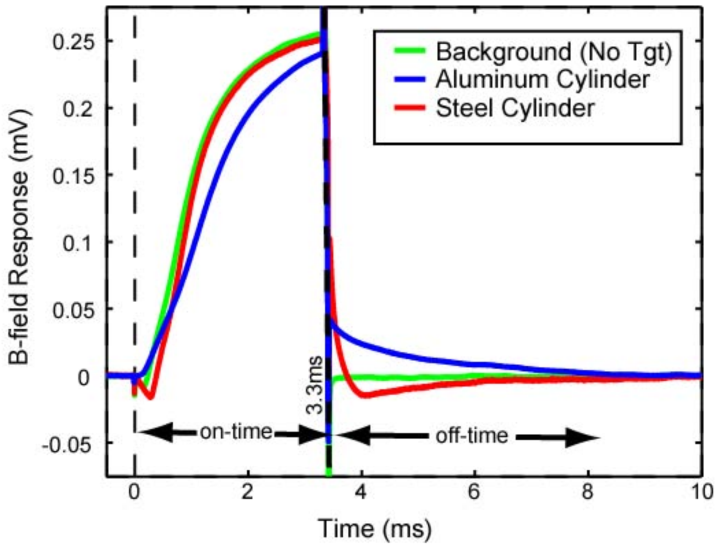

Figure 45 B-field response during excitation of the EM-61 transmitter. The total field is represented since no attempt was made to cancel the primary field. Despite the presence of the primary field, a relatively strong anomaly is observable during the on-time.

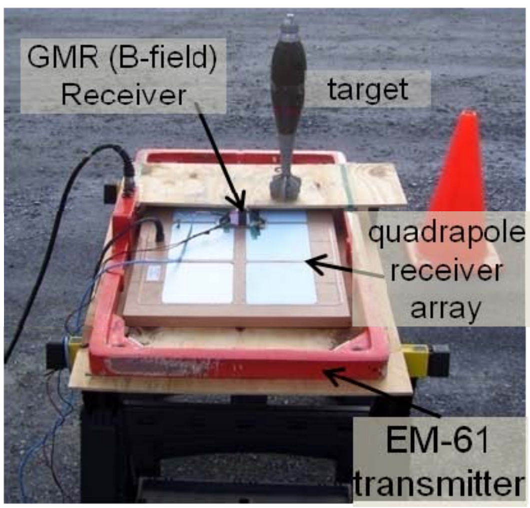

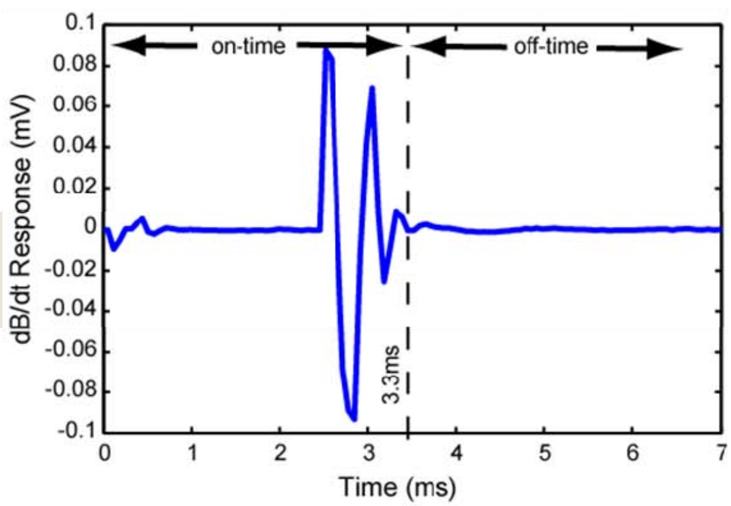

Figure 46. (left) Data collection configuration for EM-61 transmitter with quadrapole differential receiver array and GMR sensor. The quadrapole array was carefully positioned in the center of the EM-61 loop so as to effectively null the primary field from the transmitter. (right) The background signal from the center quadrapole receiver channel. The primary field during the on-time (between 0.6 and 2.4 ms) duration is nulled due to the geometry of the horizontal differential receivers.

As shown in Figure 46 (right), the primary field is effectively removed (nulled to zero) during the on-time period between 0.6 and 2.4 ms. The strong transients during ramp-on and ramp-off of the current waveform produce some residual signal. This background residual primary signal is subtracted from the receiver data when targets are present.

As shown previously, Figure 47 shows the opposing B and dB/dt signal polarity during the on-time for ferrous (steel) and non-ferrous (aluminum) objects. The offset in the B-field data before and after the on-time period is likely due to the influence of Earth's magnetic field on ferrous target. This magnetostatic (DC) excitation is similar to what is measured with a magnetometer. During the on-time, the influence of the Earth's field is superposed with the magnetostatic excitation in response to the primary magnetic field from the transmitter.

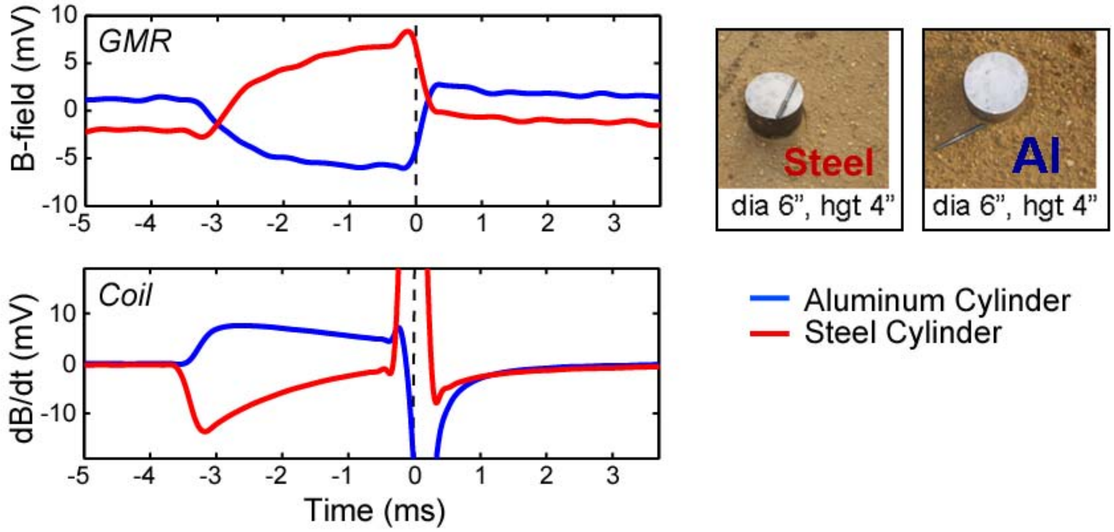

Figure 47. Responses to the EM-61 exponential ramp-on energizing waveform in the presence of ferrous (steel) and non-ferrous (aluminum) cylinders.

We repeated this measurement procedure while moving standard axi-symmetric objects and inert UXO objects over the sensor array. By sampling the B and dB/dt responses at particular times through both the on- and off-time periods we form effective target response transects. These are shown in Figure 48 (A and B) for a 37mm and 81mm UXO. Both targets display opposing on- and off-time signals. The 37mm is composed primarily of steel and thus exhibits a strong ferrous response. The 81mm is considered more of a composite object with a ferrous head and non-ferrous tail, although its signal appears to be dominated by the ferrous components in that the on- and off-time signals are strongly anti-correlated. Compiling the results for various types of UXO and a steel cylinder and copper disc, Figure 48C shows the absolute signal amplitude sampled at one position and one time for both the on- and off-time signals. The amplitudes are nearly the same for the copper disk, as a consequence of the on and off times sampled.

Traverses over the aluminum and steel cylinders are represented in Figure 49. Here we compare the on- and off--time amplitudes to the show the strong correlation of signals for the non-ferrous (aluminum) cylinder and anti-correlation for the ferrous (steel) cylinder. The differential configuration of the receiver coils yields zero signal when the target is directly under the centerpoint of the receiver pair.

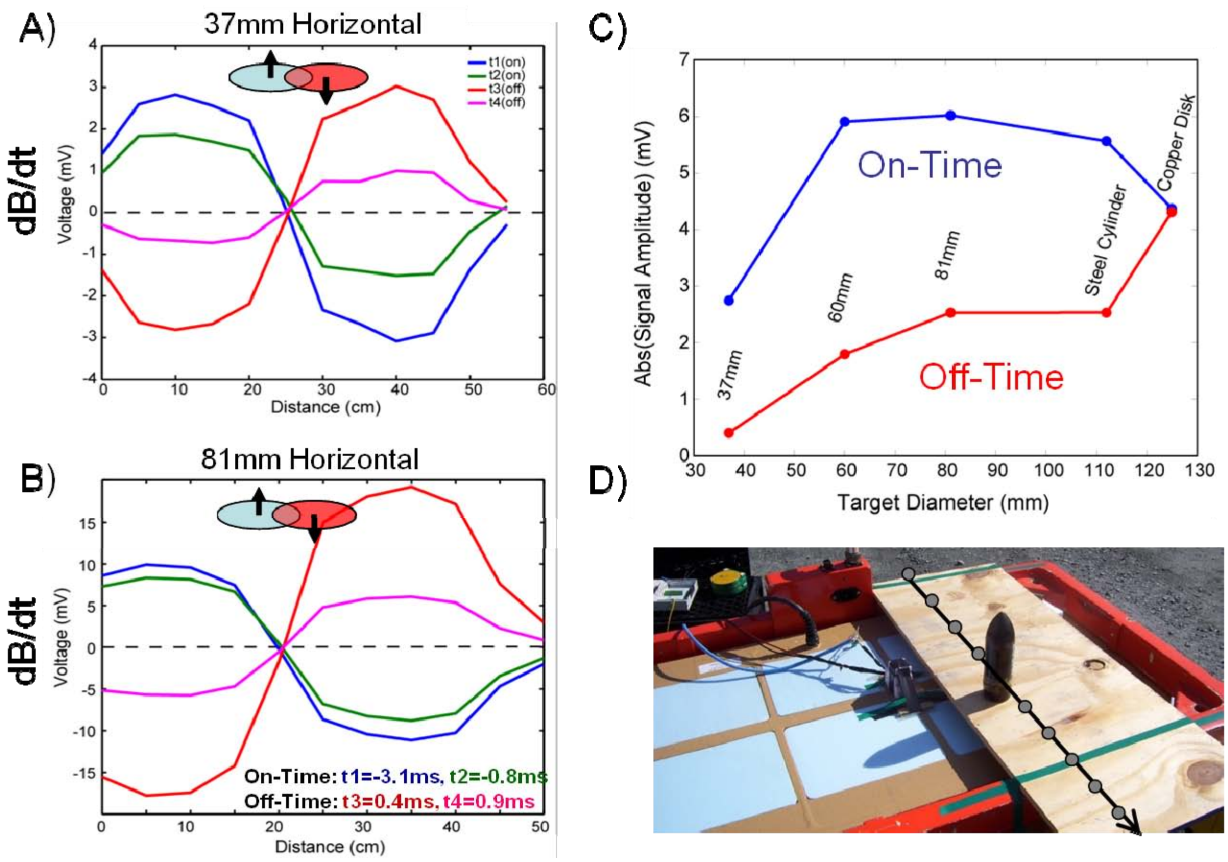

Figure 48. A) Voltage (dB/dt response) measured from the quadrapole induction coil receiver array as a 37mm projectile was placed at different positions across the EM-61 transmitter. The spatial response of the on-time data channels (blue and green) is opposing that of the off-time data channels (red and magenta). On- and off-time data channels were selected at times (t_1[on-time]=-3.1ms, t_2[on-time]=-0.8ms, t_3[off-time]=0.4ms, t_4[off-time]=0.9ms) during the respective periods such that the responses were approximately equivalent. B) Voltage (dB/dt response) from an 81mm mortar. C) Comparison of the on-time (t[on]=-3.1ms) and off-time (t[off]=0.9ms) for various types of targets. The absolute signal amplitude was retrieved from data collected while targets were placed at 15cma long the transect. D) Photograph of the data collection lay out with a 37mm target oriented vertically along the transect. The blue foam occupies the gaps in the centers of the quadrapole differential loops.

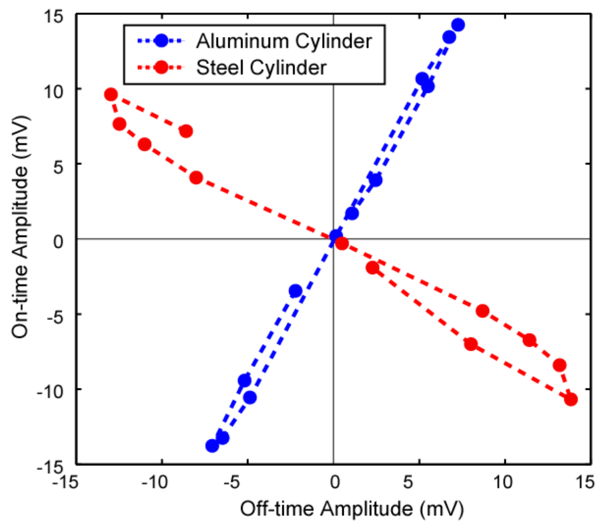

Figure 49. Comparison of the on-time and off-time signal amplitudes across a limited portion of the array. The signal amplitudes go from positive to negative across the differential receivers, with the null (essentially zero amplitude for both on- and off-time amplitudes) when the target is directly over the centerpoint between the two coils in the pair.

6.1.4. STMR Data

In order to test the veracity of full waveform models using the equivalent circuit and linear systems approaches, we performed a series of measurements with simple targets. We utilized the large moment transmitter from the Minelab STMR array along with wide-band GMR sensors to measure the magnetic field response from well-characterized coil targets. The current waveform consists of both long- (t=120us) and short-duration (t=24us) current ramps of opposite polarity. Centering the GMR magnetic field sensor in the array, we measured the response to a set of well-characterized (in terms of area, number of turns, inductance, resistance, and capacitance) shorted coil windings. The experimental set-up is shown in Figure 50A.

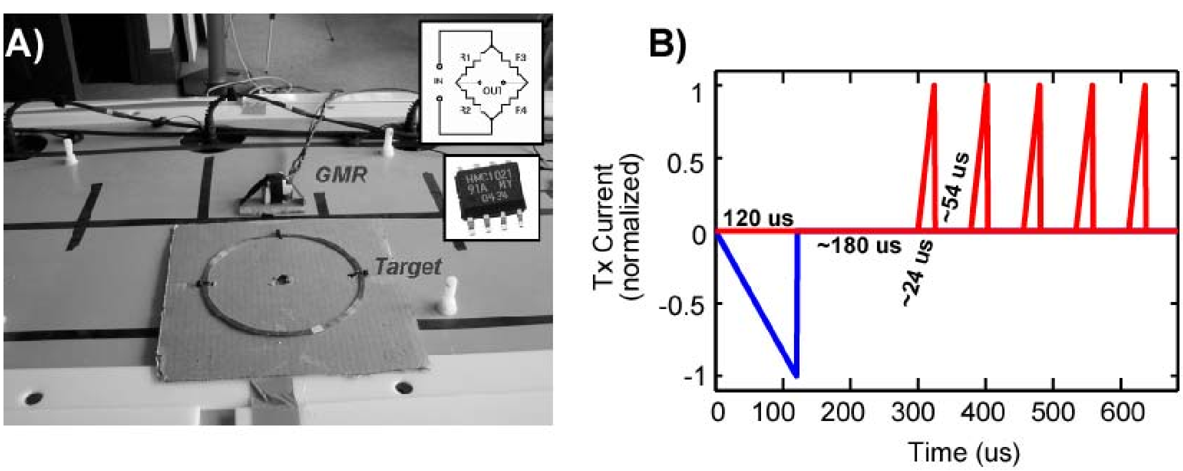

Figure 50 A) Photograph of the experimental set-up for *B* and *dB/dt* on-time laboratory measurements. B) STMR transmitter current function consisting of both long- and short-duration linear ramp waveforms.

Using the full waveform analytical model derived from equivalent circuits, we predict the response to coil targets with various time constants $\tau = L/R$. Even though the ramp-off period is affected by a parasitic transient response from the GMR circuit, we are able to predict the full waveform response for all portions of the excitation period (Figure 51). The baseline difference of ~35μV is attributed to bias in the GMR circuit.

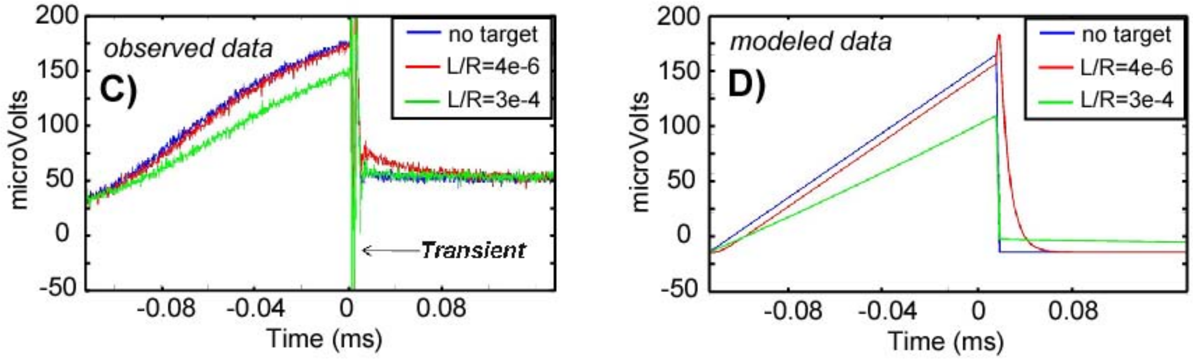

Figure 51. A) Measurements from a GMR magnetic field sensor at the center of the STMR transmitter with shorted coil windings emplaced nearby as test targets. Nonlinear bias and measurement noise in the form of a strong transient signal mask the decay during the off-time, but variations during the on-time are clearly observed. B) Results of simple circuit theory model for the full waveform response show agreement with observed data.

Data also were collected by sampling the STMR quadrapole coil receivers directly using a National Instruments data acquisition system sampling at 1.25 MHz. The horizontal gradient receiver pairs tend to null much of the primary field excitation. Figure 52 shows the response from coil windings to the shorter duration (24 μs) linear current ramp on and shut-off. The coils were placed approximately 20 cm horizontally and 15 cm vertically from the center of the receiver pairs. When the coils are positioned in vertical orientation only the background transient signal is observed. Figure 53 shows a comparison between STMR data and full waveform equivalent circuit model. Figure 54 and Figure 55 show full waveform responses for steel and aluminum cylinders, and a test grenade and 60mm projectile, respectively.

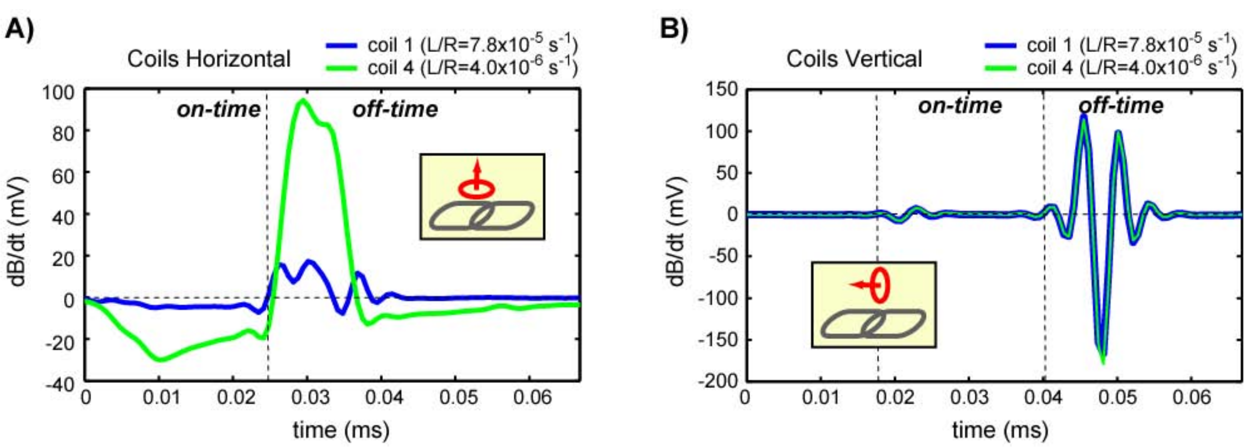

Figure 52 Full waveform STMR data collected with a National Instruments data acquisition system by sampling the differential quadrapole coils. A) Response from Coil 1 and Coil 4 oriented horizontally with corresponding characteristic time decays of 7.8×10^{-5} s^{-1} and 4.0×10^{-6} s^{-1}. B) Responses from Coil 1 and Coil 4 oriented vertically (horizontal dipole). Due to the position and geometry of the coil near the receivers there is essentially no response.

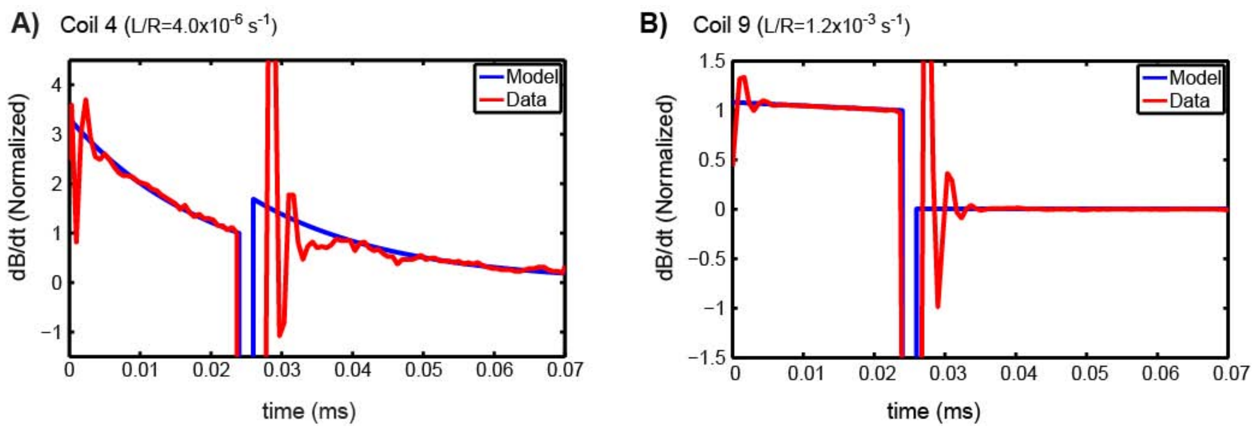

Figure 53. Comparison between STMR data and full waveform equivalent circuit model. A) Data and model fit for Coil 4. B) Data and model fit for coil 9.

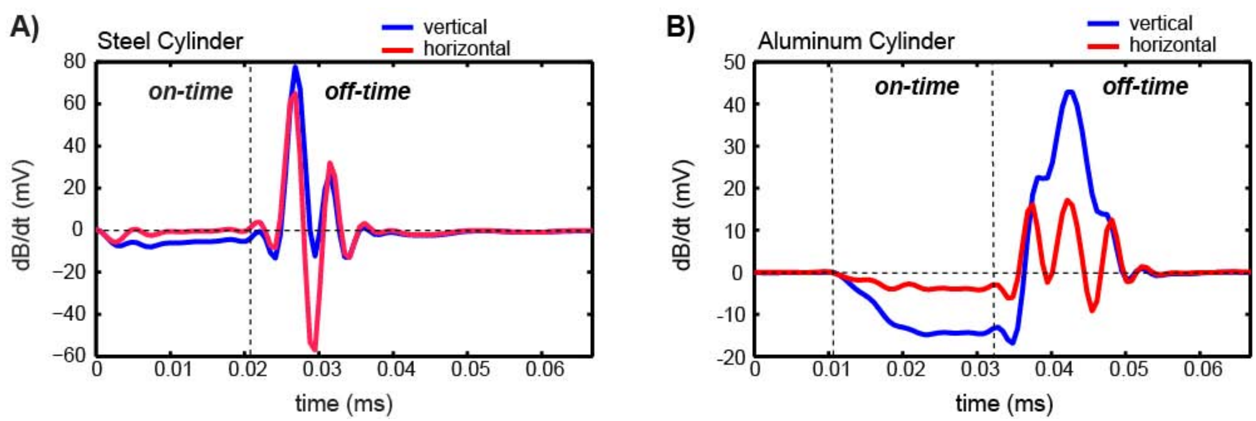

Figure 54. Full waveform responses for A) steel cylinder and B) aluminum cylinder. Although the off-time signal is difficult to interpret, the on-time signals are evident for both targets.

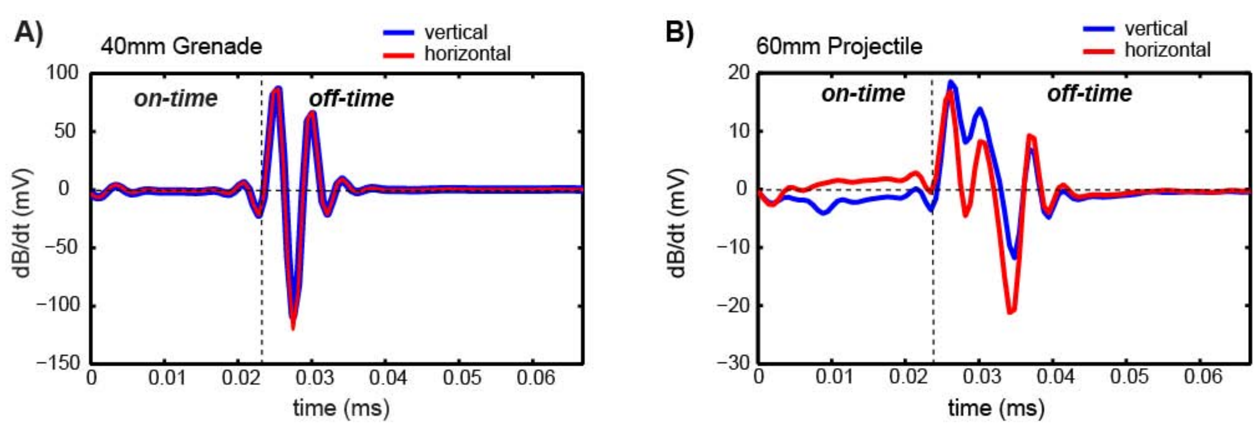

Figure 55. Full waveform responses for A) 40mm practice grenade and B) 60mm projectile. The on-time signal for the 40mm grenade is masked by the background signal, but the 60mm projectile exhibits a clear on-time response.